Macromolecules **2005,** *38,* 7521−7523 **7521**

Notes

Photorefractive Response of Polymeric Composites with Pendant Triphenylamine Moiety

Naoto Tsutsumi,* Takehiro Murao, and Wataru Sakai

Department of Polymer Science & Engineering, Kyoto
Institute of Technology, Matsugasaki, Sakyo, Kyoto
606-8585, Japan

Received May 30, 2005
Revised Manuscript Received July 1, 2005

Introduction

Information and data processing technology have been widely developed. Among them, photorefractive organic composites have high potential applications such as holographic optical devices for data storage and real-time image processing. Since the first report on photorefractive polymer composite had been published,[1] many studies of photorefractive organic materials have been investigated, which has been well reviewed in the articles.[2,3] We have also developed photorefractive response of poly(vinylcarbazole) (PVCz) composite[4] and related materials.[5,6] It was obtained the response time $t = 0.004$ s and optical gain = 31.7 cm^{-1} at 80 V/μm for the composites using tolyldiphenylamine links as the hole transporting units.[7] Large asymmetric two-beam coupling (asymmetric energy transfer), which is caused by out-of-phase refractive index modulation with respect to the illumination pattern, is a unique feature of photorefractive materials. Refractive index modulation due to photochromism, photoisomerization, thermorefraction, and photobleaching is in-phase to illumination pattern, which cannot give the asymmetric energy transfer.

In this paper, we present a newly synthesized photorefractive vinyl polymer with pendant moiety of triphenylamine, poly(4-diphenylamino)styrene (PDAS). The photorefractive performance of PDAS composites including a sensitizer, a nonlinear optical dye, and a plasticizer was investigated in comparison with that of conventional composite based on PVCz.

Experimental Part

Materials. PDAS was prepared via the synthetic method already been reported in the literature.[8] The following is a summary of synthetic route of PDAS. Triphenylphosphonium methylide was synthesized with methyltriphenylphosphonium bromide (12.5 g, 0.035 mol) and 1.6 M n-butyllithium (21.9 mL, 0.035 mol) in dehydrated tetrahydrofuran (THF) solution for 4 h under mixing. Then, adding 4-(diphenylamino)benzaldehyde (9.56 g, 0.035 mol) to this solution under mixing for 2 h, 4-diphenylaminostyrene (DAS) was synthesized via the Wittig reaction. The obtained crude DAS was purified using a column chromatography with dichloromethane as an developing solvent at room temperature. The melting point of DAS was 91.3 °C. DAS monomer (0.5 g/mL) was polymerized in tetrahydrofuran (THF) with a 2,2′-azobis(isobutyronitrile) as an initiator in a vacuum at 60 °C for 12 h to prepare PDAS. Obtained PDAS was reprecipitated in acetone. ^{1}H nuclear magnetic resonance (NMR) spectra in $\mathrm{CDCl_3}$ are as follows: δ (ppm) = 7.3−6.95 (m, 14H, Ar), 6.65 (q, 1H, CH), 5.65 (d, 2H, $\mathrm{CH_2}$), 5.15 (d, 2H, $\mathrm{CH_2}$) for DAS. δ (ppm) = 6.9 (br, 14H, Ar), 2.0 (br, H, −CH⟨), 1.55 (br, 2H, $-\mathrm{CH_2}-$) for PDAS. 2,4,7-Trinitro-9-fluorenone (TNF) was used as a sensitizer and 4-azacycloheptylbenzylidene−malononitrile (7-DCST) as a nonlinear optical dye. Diphenyl phthalate (DPP) was used as a platicizer to decrease glass transition temperature (T_g) of composites. 7-DCST was synthesized using a method in ref 9. TNF and DPP were used as received. Figure 1 shows the structural formulas of these materials.

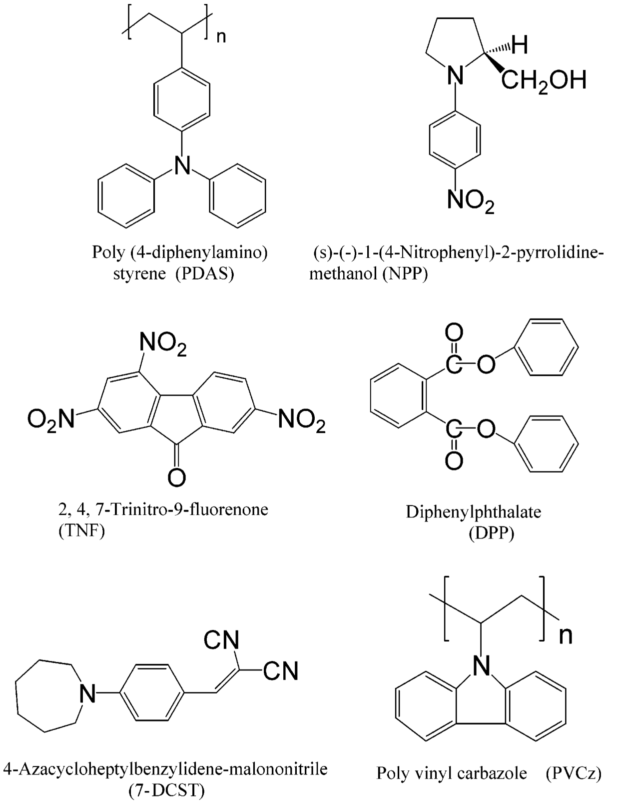
Poly (4-diphenylamino) styrene (PDAS)
(s)-(-)-1-(4-Nitrophenyl)-2-pyrrolidine-methanol (NPP)
2, 4, 7-Trinitro-9-fluorenone (TNF)
Diphenylphthalate (DPP)
4-Azacycloheptylbenzylidene-malononitrile (7-DCST)
Poly vinyl carbazole (PVCz)

Figure 1. Structural formulas of chemicals used in this study.

Sample Preparation. Composites with a given weight ratio of PDAS, TNF, 7-DCST, and DPP were dissolved in THF. Composite films were cast from THF solution and dried on a heated plate at 70 °C for 24 h and subsequently in a vacuum at 70 °C for 24 h. Dried composites were melt-pressed between two indium−tin oxide (ITO) glass plates with a proper spacer. Film thickness was ca. 50 or 100 μm.

Four-Wave Mixing Diffraction Measurement. Diffraction grating of the sample film was measured using a degenerate four-wave mixing (DFWM) technique. Holographic grating was written by p-polarized two beams of He−Ne laser (λ = 632.8 nm, 10 mW) intersected in the sample. Two writing

---

* To whom all correspondence should be addressed: Fax (+81)-75-724-7805; e-mail tsutsumi@kit.ac.jp.

10.1021/ma051113b CCC: $30.25

Table 1. Absorption Coefficient, Photocurrent, and Refractive Index at 632.8 nm for Each Composite

	absorption coefficient (cm^{-1})	photocurrent ($\mu A/(W\ cm^2)$)	refractive index
PDAS 39	21.6	1.45	1.6638
PDAS 39.5	14.7	0.55	1.6664
PDAS 49	22.8	1.26	1.6529
PVCz 49	22.9	0.11	1.6842

beams intersect in the sample at incidence angles of $\alpha_A = 40.54°$ and $\alpha_B = 59.46°$ in air. The s-polarized reading (probe) beam from the same source propagates in the direction opposite to one of the writing beams (beam B) is diffracted by the photorefractive grating in the sample film, and the diffracted signal propagates in the direction opposite to that of beam A and is reflected off by a beam splitter. The diffracted signal is then detected by a photodiode detector.

Two-Beam Coupling Measurement. Photorefractive coupling gain coefficients of the sample were measured using the two-beam coupling (2BC) technique with p-polarized He−Ne laser ($\lambda = 632.8$ nm, 10 mW). The same geometric configuration of p-polarized two beams crossing as DFWM was used except that no probe beam was used. The intensity of two crossing beams were measured using photodiode detectors to evaluate gain coefficients (optical gain).

Characterization. The NMR spectrum was measured with TMS as an internal standard at 20 °C using a Varian model Gemini-200. The number-average molecular weight (M_n) and weight-average one (M_w) of PDAS were measured using a gel permeation chromatograph, Shodex GPC SYSTEM-21, with a serially connected columns of G5000Hxl and G3000Hxl. The UV−vis absorption spectrum was recorded on a Shimadzu UV-2101PC spectrophotometer. Differential scanning calorimetry was carried out on a TA Instruments DSC 2920 differential scanning calorimeter with a heating rate of 10 °C/min to determine the glass transition temperature of sample. The m-line method, in which an evanescent field is responsible for the guided-wave mode at discrete mode angle, was employed to determine refractive indices of sample films. The laser source is a polarized He−Ne laser (632.8 nm). A prism of TaFD21 (HOYA Glass) with high refractive index (1.92588 at 632.8 nm) was coupled to film with an air gap. Photoconductivity was measured using an electrometer at applied voltage of 400 V under an illumination of monochromated xenon light. Electrooptic measurement was performed with a He−Ne laser to determine Pockels coefficient at $\lambda = 632.8$ nm.

Results and Discussion

Four different PDASs with different M_n of 5000, 9000, 14 000, and 20 000 with ratio of M_w/M_n of 2.3, 2.2, 1.6, and 1.6, respectively, were synthesized. Glass transition temperatures of PDAS are 142.6, 141.3, 140.4, and 134.7 °C in turn as decreasing molecular weight. Composites of PDAS with lowest molecular weight gave the best quality film for photorefractive performance. Then PDAS with M_n of 5000 was used in the present work.

Four types of sample films were prepared. PDAS/7-DCST/DPP/TNF (39/15/45/1), PDAS/7-DCST/DPP/TNF (39.5/15/45/0.5), PDAS/7-DCST/DPP/TNF (49/10/40/1), and PVCz/7-DCST/DPP/TNF (49/10/40/1) were prepared and denoted as PDAS 39, PDAS 39.5, PDAS 49, and PVCz 49, respectively. PVCz 49 was prepared in comparison with the present newly synthesized PDAS composites.

Table 1 summarizes the absorption coefficient, photocurrent, and refractive index (n) at 632.8 nm for each composite. It is noted that PDAS composite gave more than 10 times as much photocurrent as PVCz one does. Photoconductive responses after a step illumination of monochromated xenon light for PDAS and PVCz composites are shown in Figure 2. The PDAS composite gave a faster photoconductive response. The faster response and larger photocurrent of PDAS composite suggest the faster drift mobility of hole in PDAS composite due to lower ionization potential of triphenylamine moiety in PDAS. Larger TNF content also leads to the larger photocurrent. These photoconductive properties of PDAS contribute to the good photorefractive properties.

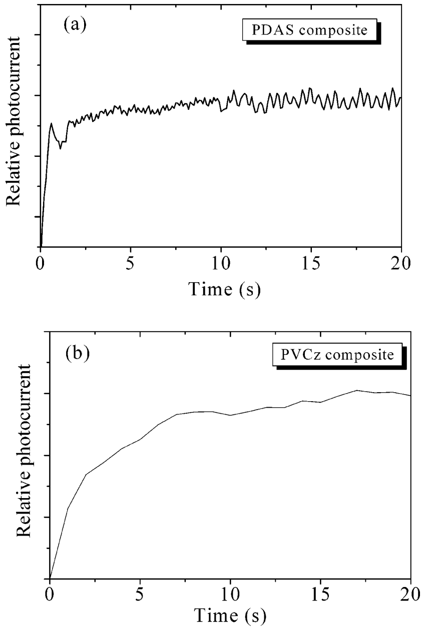

Figure 2. Time profile of photocurrent for PDAS and PVCz composites after a step illumination of manochromated xenon light. Photoillumination starts at time = 0.

Figure 3 shows the dependence of diffraction efficiency on applied electric field for each composite. Increase of applied electric field leads to the increase of diffraction efficiency. It is shown that the higher diffraction efficiency is measured for composite with higher TNF content. This result shows the larger content of charge transfer complex due to increase of TNF content is directly related to the larger space-charge field for higher diffraction efficiency.

The observed grating buildup dynamics is given by a exponential function of the kind $\eta = \eta_0[1 - \exp(-t/\tau_\eta)]$. Table 2 summarizes the diffraction efficiency (η_0), grating buildup time (τ_η), and optical gain (Γ_0). As shown in Table 2, compared with the PVCz composite, the PDAS composite has a faster response of beam diffraction. PDAS 39 has a faster response time of 0.4 s, whereas PVCz 49 has a slower response time of 1.2 s at the same applied electric field. These faster responses are also ascribed to faster drift mobility of hole in PDAS composite due to lower ionization potential of the triphenylamine moiety in PDAS.

Refractive index modulation is calculated from the diffraction efficiency for transmission grating geometry using an equation of

$$\eta_s = \sin^2[K\Delta n_s \cos \theta_G] \qquad (1)$$

where $K = \pi d/\lambda(\cos \theta_A \cos \theta_B)^{1/2}$, Δn_s is refractive index modulation, θ_G is the angle between direction of grating vector and applied electric field, d is film thickness, λ is wavelength of laser beam (= 632.8 nm), and θ_A and θ_B are internal refraction angles of beam A and beam B in the film, respectively.

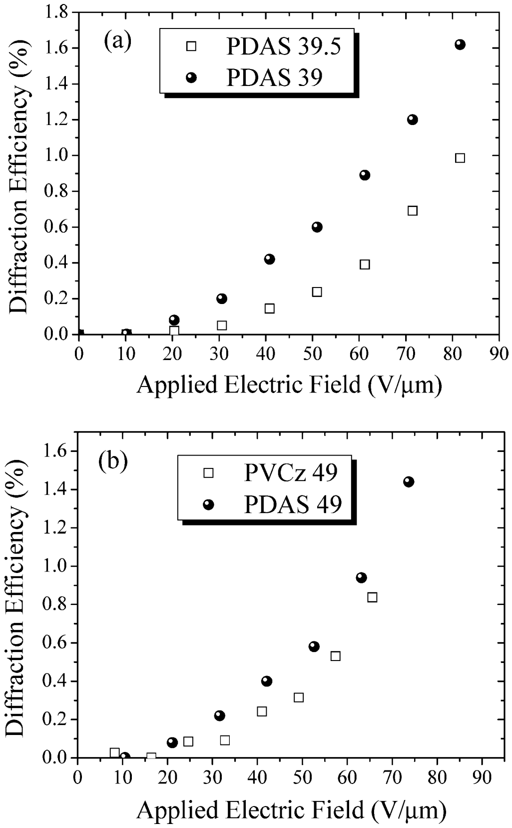

Figure 3. Diffraction efficiency as a function of applied electric field: (a) PDAS 39 and PDAS 39.5; (b) PDAS 49 and PVCz 49.

Table 2. Photorefractive Parameters Obtained DFWM and 2BC Measurements

	E_0 (V/μm)	η_0 (%)	τ_η (s)	Γ_0 (cm^{-1})
PDAS 39	61.2	0.89	0.4	20.5
PDAS 39.5	61.2	0.39	0.9	12.4
PDAS 49	63.2	0.94	0.7	14.1
PVCz 49	65.6	0.83	1.2	11.0

Table 3. Electrooptic Coefficient, Refractive Index Modulation, Space-Charge Field, and Photorefractive Phase Shift in the Matrix

	E_0 (V/μm)	r_{33} (pm/V)	Δn_s	Ψ (deg)
PDAS 39	61.2	2.2	3.9×10^{-4}	90
PDAS 39.5	61.2	2.0	2.6×10^{-4}	74
PDAS 49	63.2	1.5	4.0×10^{-4}	45
PVCz 49	65.6	1.8	2.9×10^{-4}	50

The phase shift, out-of-phase refractive index modulation with respect to the illumination pattern, is a unique feature of photorefractive effect in the devices. The phase shift of Ψ is evaluated from the refractive index modulation (Δn) and optical gain (Γ_0) with an eq 2[10]

$$\Gamma_0 = \frac{\pi \Delta n}{\lambda}(\hat{e}_1 \cdot \hat{e}_2) \sin \Psi \tag{2}$$

where $\hat{e}_i$ are the polarization vectors of the incoming beams. The standard model of the photorefractive effect developed for inorganic materials predicts the 90° phase shift. As seen in Table 3, PDAS 39 showed 90° phase shift and PDAS 39.5 showed 74° ($\sin 74° = 0.96$), which is almost close to 90°. PDAS 49 and PVCz 49 showed the phase shift of 45° and 50°, respectively. A smaller phase shift, large deviation from 90°, has been reported in many polymeric composites. The main reason for the smaller phase shift is ascribed to the fact that the photorefractive mechanism in polymeric composites is based on the external electric field dependence of carrier mobility and trap densities. In the standard Kukhtarev model, if large trap densities are assumed, smaller values of the phase shift will be obtained.[11] Cyclic volutammetry showed that 7-DCST has oxidation potential of 1.49 V (vs Ag/AgCl electrode) lower than 1.66 V for ethylcarbazole as a model compound of PVCz. Triphenylamine as a model compound of PDAS has oxidation potential of 1.38 eV. The lower oxidation potential means lower ionization potential. The lower ionization potential of 7-DCST suggested that 7-DCST works as a hole trap in PVCz composite but not in PDAS composite. This is consistent with the smaller photocurrent and slower response of photoconductivity in PVCz composite and larger photocurrent and faster response of photoconductivity in PDAS composite. 7-DCST does not work as any trap sites in PDAS composite.

Conclusion

Photorefractive properties of newly synthesized PDAS as a triphenylamine pendant moiety have demonstrated. Better photoconductive properties such as large photocurrent and fast photoconductive response of PDAS composites are consistent with their better photorefractive response. This approach provides one of the promised candidates of the future holographic data optical storage memory.

Acknowledgment. The authors thank Dr. Nishio, Core Technology Center, Nitto Denko Corporation, Japan, for the special gift of 7-DCST. N.T. also thanks Mr. Nakajima for measuring cyclic volutammetry of 7-DCST, triphenylamine as model compound of PDAS, and ethylcarbazole as PVCz.

References and Notes

(1) Ducharme, S.; Scott, J. C.; Twieg, R. J.; Moerner, W. E. *Phys. Rev. Lett.* **1991**, *66*, 1864.
(2) Moerner, W. E.; Silence, S. M. *Chem. Rev.* **1994**, *94*, 127.
(3) Ostroverkhova, O.; Moerner. W. E. *Chem. Rev.* **2004**, *104*, 3267.
(4) Tsutsumi, N.; Shimizu, Y. *Jpn. J. Appl. Phys.* **2004**, *43*, 3466.
(5) Nishio, A.; Wasai, K.; Tsutsumi, N. *Kobunshi Ronbunshu* (in Japanese) **2003**, *60*, 725.
(6) Tsutsumi, N.; Eguch, J.; Sakai, W. *Chem. Phys. Lett.* **2005**, *408*, 269.
(7) Park, S.-H.; Ogino, K.; Sato, H. *Synth. Met.* **2000**, *113*, 135.
(8) Hattemer, E.; Brehmer, M.; Zentel, R.; Mecher, E.; Müller, D.; Meerholz, K. *Polym. Prepr.* **2000**, *41*, 785.
(9) Diaz-Garcia, M. A.; Wreight, D.; Casperson, J. D.; Smith, B.; Glatzer, E.; Moerner, W. E.; Sukhomlinova, L. I.; Twieg, R. J. *Chem. Mater.* **1999**, *11*, 1784.
(10) Yariv, A. *Optical Electronics in Modern Communications*; Oxford University Press: Oxford, 1997; p 683.
(11) Hendrickx, H.; Wang, J. W.; Maldonado, J. L.; Volodin, B. L. Sandalphon; Mash, E. A.; Persoons, A.; Kippelen, B.; Peyghambarian, N. *Macromolecules* **1998**, *31*, 734.

MA051113B